

# IMAgent: Training Multi-Image Vision Agents via End2End Reinforcement Learning

Chengqi Dong<sup>1,2</sup>, Chuhuai Yue<sup>1</sup>, Hang He<sup>1</sup>, Rongge Mao<sup>2</sup>, Fenghe Tang<sup>2</sup>, S Kevin Zhou<sup>2</sup>, Zekun Xu<sup>1</sup>, Xiaohan Wang<sup>1</sup>, Jiajun Chai<sup>1</sup>, Wei Lin<sup>1</sup>, Guojun Yin<sup>1</sup>

<sup>1</sup> MeiTuan, <sup>2</sup> University of Science and Technology of China

## Abstract

*Recent VLM-based agents aim to replicate OpenAI O3’s “thinking with images” via tool use, but most open-source methods limit input to a single image, falling short on real-world multi-image QA tasks. To address this, we propose IMAgent, an open-source vision agent trained via end-to-end reinforcement learning dedicated for complex multi-image tasks. By leveraging a multi-agent system, we generate challenging and visually-rich multi-image QA pairs to fully activate the tool-use potential of the base VLM. Through manual verification, we obtain MIFG-QA, comprising 10k samples for training and evaluation. With deeper reasoning steps, VLMs may increasingly ignore visual inputs. We therefore develop two specialized tools for visual reflection and confirmation, allowing the model to proactively reallocate its attention to image content during inference. Benefiting from our well-designed action-trajectory two-level mask strategy, IMAgent achieves stable tool use behavior via pure RL training without requiring costly supervised fine-tuning data. Extensive experiments demonstrate that IMAgent maintains strong performance on existing single-image benchmarks while achieving substantial improvements on our proposed multi-image dataset, with our analysis providing actionable insights for the research community. Codes and data will be released soon.*

## 1. Introduction

The agentic reinforcement learning (RL) paradigm [16, 17, 34] enables end2end training of LLM-based agents, transforming language model services from passive response generators into proactive decision-makers [1, 59]. In the vision domain, OpenAI’s O3 [29] demonstrates how interleaved chains of textual and visual reasoning can transcend the limitations of pure VLMs that merely “see” images, enabling true “thinking with images”—a novel inference behavior that significantly expands model capabilities.

Motivated by this breakthrough, many open-source efforts develop VLM-based agents (vision agents), integrating external visual processing tools with the multimodal understanding of base VLM [9, 35, 46, 63, 67]. By interleaving tool outputs with generated text tokens, these systems partially replicate O3’s advanced reasoning patterns and improve performance on complex tasks.

However, current vision agents are primarily trained to use tools in single-image scenarios [3, 36, 46, 63, 67]. Multi-image tasks require explicit identification and indexing of target images for each operation; thus, directly transferring such models to multi-image settings often fails to meet real-world demands where multi-image understanding is common and essential [25]. On the other hand, existing work focuses mainly on stabilizing tool use, either by carefully curating trajectory data for supervised fine-tuning (SFT) [43], modifying RL algorithms [3, 46, 67], or combining both approaches [35, 36, 63]. Few studies investigate the underlying principles through which tool use actually enhances agent performance.

To address these issues, we develop IMAgent, the first vision agent trained end2end via agentic RL that can dynamically explore multi-image inputs and solve highly complex visual tasks.

Recognizing that existing multi-image datasets do not sufficiently elicit autonomous tool use behaviors from models, we design a collaborative multi-agent pipeline for data curation. We curate visually rich samples from both natural image [22] and scientific chart [31] datasets; generate diverse questions; conduct rigorous manual filtering; and ultimately construct approximately 10k fine-grained QA pairs (9k for training and 636 for evaluation).

Empirical analysis reveals that, without active tool use during chain-of-thought(CoT) reasoning, the model’s attention to input images gradually diminishes, especially in multi-image scenarios. As shown in Figure 1, token-level focus on image content drops to near zero in later inference stages. To mitigate this issue, we introduce two specialized tools—a zoom\_in cropping module (visual confirmation) and an image lookback\_reuse module (visual reflec-

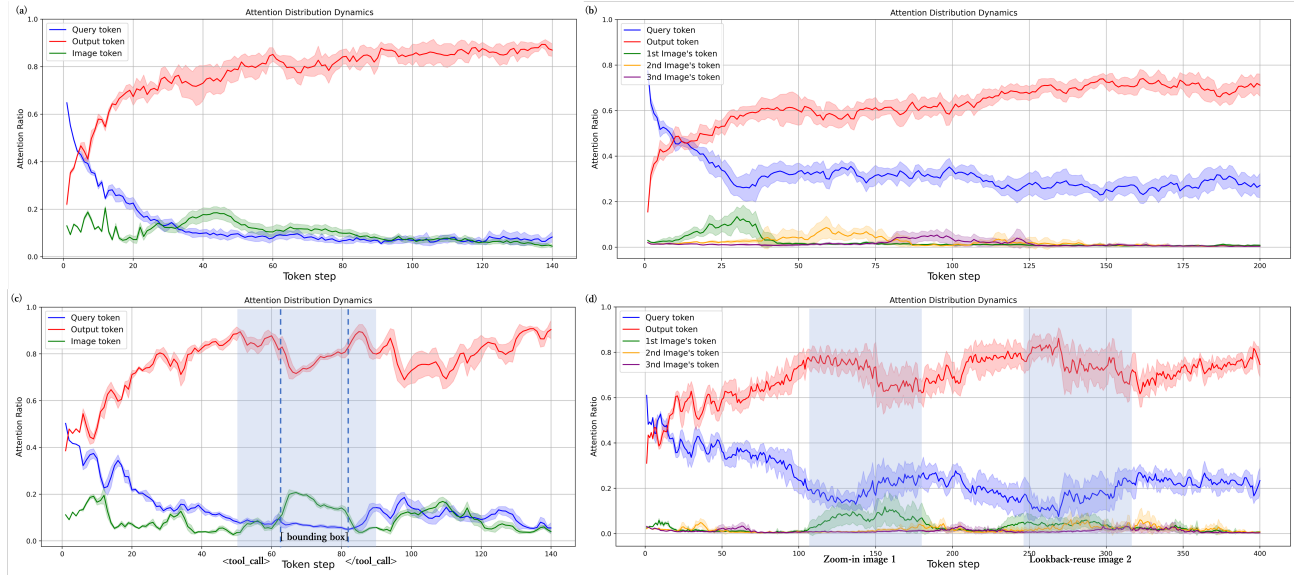


Figure 1. We compared the attention proportions of newly generated tokens by Qwen2.5-VL-7B (a, b) and IMAgent (c, d) to the input text, image tokens, and previously generated tokens as inference progresses, under single-image input (a, c) and multi-image input (b, d). Qwen2.5-VL-7B’s attention to image tokens gradually decreases and approaches zero under multi-image input (b); in contrast, IMAgent (c, d), aided by tool use, maintains dynamic visual attention throughout, even with a reasoning chain twice as long.

tion), which enable IMAgent to autonomously reallocate attention across relevant regions throughout inference while fostering human-like iterative visual thinking processes.

To avoid costly manual construction of high-quality SFT data while ensuring robust learning dynamics in complex environments, we adopt pure end2end RL training augmented by an action-trajectory two-level mask strategy designed to prevent ineffective trajectories or environment feedback from hindering exploration into advanced forms of visual reasoning. In addition, extensive experiments systematically analyze factors such as tool type that affect the behavior of vision agents during training.

In summary, our main contributions are threefold:

- We propose IMAgent, the first vision agent aimed at complex single and multi image tasks via end2end RL with MIFG-QA, a multi-image fine-grained dataset we create.
- To enable dynamic adjustment of image attention throughout reasoning, we design visual reflection and confirmation tools for IMAgent.
- Extensive experiments show that IMAgent stably uses tools and thinks with images, achieving SOTA results on single and multi-image benchmarks while providing practical training guidelines for the community.

## 2. Related Work

### 2.1. Multi-modal Reasoning Models

Multimodal reasoning models show a promising trend toward unifying multiple modalities within a language-centric

framework[23]. Early works[50, 51, 54] focus on enhancing CoT reasoning through SFT and planning algorithms like Monte Carlo Tree Search[49], improving interpretability and reliability. Building on these foundations, RL-based methods shift the paradigm from imitating static reasoning patterns to actively optimizing them via feedback. Pioneering methods[6, 55, 61] apply Direct Preference Optimization[30] for behavioral alignment. After the success of Deepseek-R1[5], Group Relative Policy Optimization (GRPO)[32] becomes a mainstream algorithm, and Reinforcement Learning with Verifiable Rewards (RLVR) emerges as a powerful new training paradigm. These methods rapidly expand from mathematical and geometric reasoning[28, 58, 68] to visual skills[26, 27, 42], and further to modalities such as video[8] and audio[66]. Their success highlights the importance of high-quality reward signals, making data augmentation[24, 48], reward design[44, 52, 60, 65] and other modifications[13, 57] central to performance. Ultimately, RLVR drives breakthroughs in reasoning depth, coherence, and domain adaptability, laying a foundation for training advanced vision agents.

### 2.2. Vision Agents

Vision Agents aim to break the limitations of static, parameterized knowledge by autonomously using tools, deeply integrating dynamic visual perception with action-based reasoning[4]. Early approaches relied on prompt engineering to passively trigger tools[10, 15, 38, 56], while current

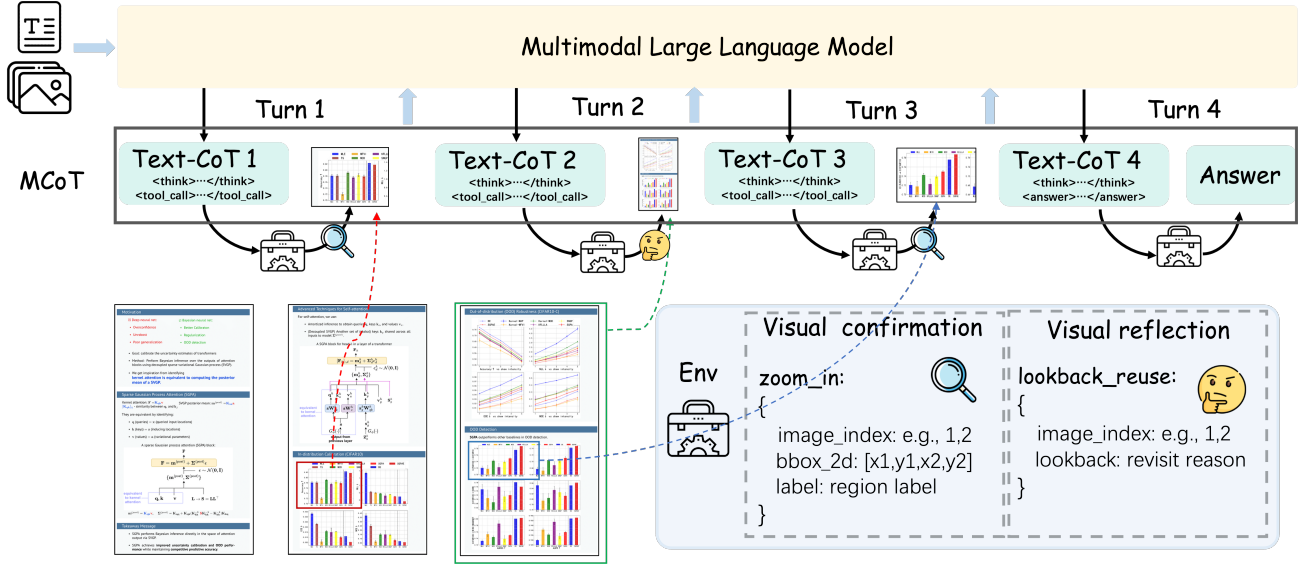


Figure 2. Figure 2: Overview of IMAgent. Our model will automatically choose whether and how to use tools based on the actual problem. Visual verification is achieved by cropping local regions of the image using `zoom_in`, and visual reflection is achieved by reusing the input image using `lookback_reuse`.

mainstream methods increasingly adopt RL post-training, driving advances in multimodal retrieval[11, 40, 45] and integrated code execution[7, 12, 21, 39]. Notably, OpenAI’s O3 and Qwen3-VL[37] enable models to “think with images”, generating intertwined chains of thought that combine text and visuals. Inspired by O3’s great performance, many open-source solutions have emerged[3, 18, 35, 62, 63, 67], typically adopting a two-stage post-training process: SFT for tool call format learning, followed by RL to enhance visual tool use for complex tasks. However, this approach requires carefully curated SFT datasets and limits generalization. Deepeyes[67] cultivates tool-calling ability through pure reinforcement learning, but is limited to single image input and a single tool type. Though, aforementioned works achieve partial power of O3, they mainly focus on reproducing the tool use ability in single-image scenarios, largely neglecting the more common multi-image input settings. Addressing this gap is one of the main motivations of our work.

### 3. Method

#### 3.1. Reasoning Pattern

Our goal is to train a vision agent capable of complex multi-image tasks through end2end reinforcement learning. Equipped with confirmation and reflection capabilities, IMAgent can autonomously verify local details and revisit the global context, fostering a dynamic visual reasoning process. Even in late-stage inference, the agent maintains a high degree of attention to the image and acquires requisite

information via attention refocusing driven by visual confirmation and attention redistribution driven by visual reflection.

Adhering to a dynamic “think–act–iterate” paradigm, IMAgent outputs the final answer after obtaining sufficient information. Specifically, the workflow proceeds as follows:

- Initial Reasoning.** Given an image set  $I$  and a corresponding question  $Q$ , IMAgent performs an initial reasoning step. During this stage, the model autonomously decides whether to invoke visual confirmation or reflection. If the model calls a tool, it will output structured tool use tags.
- Visual Functions.** When a visual function is triggered, the model emits the function type and its arguments. For *visual confirmation* via local image cropping, the model outputs an image index to specify the target image, a bounding box to indicate the region to zoom in on, and a label to emphasize the region of interest. For *visual reflection* via image reuse, the model outputs an image index and a reflection reason, which reinforces the purpose of reflection and enhances logical interpretability.
- Process Reasoning.** The returned results are concatenated with the historical trajectory in an appropriate format, forming the input for the current step. The model continues reasoning based on this augmented trajectory.
- Iteration.** IMAgent repeats Steps 2–3 until it either reaches the maximum interaction limit or produces an answer, at which point inference terminates.

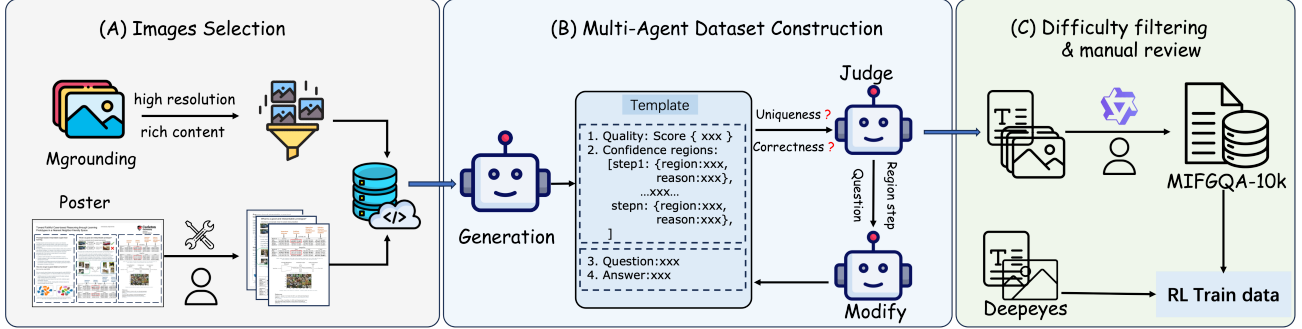


Figure 3. A three-stage data construction pipeline based on multi-agent systems.

### 3.2. Curation of MIFG-QA

To train the model’s dynamic visual reasoning capabilities for multi-image tasks, we design a three-stage data synthesis pipeline (as shown in Figure 3).

**Stage 1: Images Selection.** Considering the necessity of activating visual capabilities, we exclude low-resolution images and selected data with rich visual content. Specifically, for natural images, we randomly sample high-resolution data from MGrounding [22], covering image groups with relationships such as difference, contrast, and time. For scientific figures, we construct the dataset from high-resolution conference posters [31]. We perform adaptive structural segmentation on individual conference posters, treating different segmented regions as multi-image data. The resulting multi-image dataset maintains strong contextual relevance.

**Stage 2: Multi-Agent Data Construction.** First, a question generation agent is asked to generate fine-grained QA pair according to the given original images. To ensure the high quality and credibility of the generated questions, the Agent is also required to output structured reasoning steps from questions to answers, including confidence regions and reasoning details. Subsequently, an Answer Verification Agent evaluates the uniqueness of answers and the correctness of reasoning logic based on the questions and reasoning steps. If the criteria are not met, a Question Revision Agent is activated to iteratively refine the questions until the requirements are satisfied.

**Stage 3: Quality Filtering and Difficulty Calibration.** To ensure the training data has appropriate difficulty, We perform five rollouts on the entire dataset using Qwen2.5-VL-7B to select samples of moderate difficulty, removing samples that are too difficult or too simple. Then, we conduct further rule-based screening and invite several human experts to conduct manual quality checks to ensure the quality of the training data. More information on data construction is provided in the appendix.

We ultimately obtain approximately 10k samples, with an average total pixel count per question of 3 million (for

natural images) and 9 million (for poster images). From this, we derive MIFG-QA-val, a benchmark for evaluating models’ multi-image multi-hop fine-grained reasoning abilities. Combined with Deepeyes single-image data, this dataset serves as the training data for IMAgent.

### 3.3. End2End Reinforcement Post-training

We employ an end2end reinforcement learning framework to train the model. The core objective is to cultivate the model’s dynamic visual reasoning ability—that is, to adaptively optimize tool invocation decisions based on multi-turn feedback, reallocate visual attention, and ultimately achieve a visual agent integrating multi-turn tool inference. We use the GRPO algorithm to optimize the parameterization strategy  $\pi_\theta$ , enabling the visual agent to maximize the expected cumulative reward of the task by dynamically adjusting the lexical generation logic, while removing KL regularization.

#### 3.3.1. Reward Shaping

We design both result rewards and format rewards, with an additional tool use gain incorporated into the result rewards to incentivize the model’s exploration and utilization of tools.

- **Result Reward:** Evaluated via rule-based judgment or an LLM judge, with a binary reward of 0 or 1.
- **Format Reward:** Assesses whether the model output meets all specified criteria through rule checking (e.g., completeness of tags, absence of overlap between tags). It is designed as a gradient reward, where non-compliance results in corresponding score deductions.

The total reward is defined as:

$$R(\tau) = R_{\text{acc}} \cdot (a + b \cdot \text{Tool}_{\text{gain}}) + c \cdot R_{\text{format}}$$

where  $\text{Tool}_{\text{gain}}$  represents a tool use gain (an indicator function for tool use) specifically introduced for the accuracy reward. This gain encourages the agent to obtain additional rewards through tool use under the Zero RL paradigm.

Table 1. Results of different models on various benchmarks.

Model	E2E	Param	V*			HR-Bench			MME	MIFG-QA		
			direct	relative	Avg	4K	8K	Avg		nature	poster	Avg
GPT-4o [14]	–	–	–	–	66.0	59.0	59.0	59.0	45.2	49.26	47.55	48.11
SEAL [47]	✗	7B	–	–	75.4	–	–	–	–	–	–	–
Dyfo [20]	✗	7B	–	–	81.2	–	–	–	–	–	–	–
Zoomeye [33]	✗	7B	93.9	85.5	90.6	69.6	69.3	69.45	–	–	–	–
LLaVA-OneVision [19]	–	7B	75.7	75.0	75.4	63.0	59.8	61.4	57.4	37.93	39.49	38.99
Qwen2.5-VL [2]	–	7B	79.13	73.68	76.96	70.62	66.75	68.69	57.3	36.94	44.34	41.98
Qwen2.5-VL-CoT [2]	–	7B	73.91	76.32	74.86	68.5	62.25	65.38	59.63	36.35	40.65	39.31
Chain-of-Focus [63]	✗	7B	–	–	88.0	–	–	–	–	–	–	–
Deepeyes [67]	✓	7B	<u>90.43</u>	<u>84.21</u>	<u>87.96</u>	<b>75.0</b>	<u>69.75</u>	<u>72.38</u>	64.0	38.75	43.84	38.36
Pixel Reasoner [35]	✗	7B	<b>91.3</b>	77.63	85.86	68.75	63.25	66.0	<u>64.41</u>	<u>41.87</u>	<u>45.72</u>	<u>44.49</u>
IMAgent	✓	7B	88.70	<b>88.16</b>	<b>88.48</b>	<u>73.5</u>	<b>71.5</b>	<b>72.5</b>	<b>64.83</b>	<b>50.24</b>	<b>48.73</b>	<b>49.21</b>

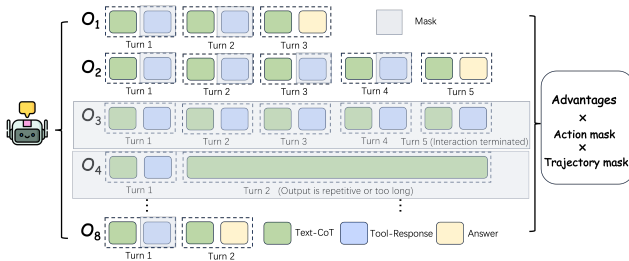


Figure 4. Action-Level and Trajectory-Level Mask.

### 3.3.2. Two-Level Mask Strategy

To adapt to the training of visual tools, we design a two-level mask strategy to enhance training stability (as illustrated in Figure. 4).

**Action-Level Mask.** After the model issues a tool call request, the execution results of the tool (including the execution status and returned images) are concatenated into the previous context and used as input for the next round of reasoning. However, since this information often deviates from the distribution of existing knowledge, it can lead to abnormal directions in parameter optimization. To mitigate this issue, we apply a mask to information other than the model’s output to prevent it from participating in policy updates.

**Trajectory-Level Mask.** Xue et al. [53] propose that the instability in multi-turn tool-integrated reasoning training within pure text CoT stems from the emergence and accumulation of low-probability tokens, causing distribution shifts in subsequent model outputs and generating invalid trajectories. We observe a similar phenomenon in multi-modal CoT and therefore design trajectory-level mask to filter invalid trajectories.

Specifically, we evaluate  $N$  trajectories generated by one sample in the GRPO algorithm; if a trajectory is deemed invalid, the entire trajectory is masked to exclude it from pol-

icy updates. This approach incurs almost no additional resource consumption as it directly masks generated trajectories instead of generating new valid ones. In this work, trajectories exceeding the maximum number of iterations, exceeding the maximum response length (potentially caused by repetitive model outputs), or producing no answers are classified as invalid. This mask also avoids reward-induced suppression of the model’s long-range exploration.

## 4. Experiments

### 4.1. Experimental Setup

**Hyperparameters.** We adopt an end2end reinforcement learning algorithm, GRPO, with Qwen2.5-VL-7B-Instruct as the base model. The average number of pixels per sample in our MIFG-QA (poster) exceeds 9 million, which occupies over 12k context tokens. We therefore set the maximum pixel budget to 4 million. This preserves context space to accommodate more interaction turns. The model is trained on H20 GPUs with a batch size of 256, 8 rollouts per prompt, and a maximum limit of 5 tool interactions. The KL coefficient is set to 0.0, with the maximum input length restricted to 10,480 tokens and the maximum response length to 20,480 tokens. Our single-image training data is sourced from Deepeyes, which includes fine-grained data of natural images and scientific figures, as well as reasoning data. To enable integrated reasoning over multi-image inputs, we incorporate the constructed MIFG-QA dataset. Main experimental results are presented in Table 1, where the values are the average of three independent experiments conducted with the temperature set to 0, and the maximum pixel limit of input images is 16384×28×28.

**Baselines and Benchmarks.** We conduct a systematic comparison of IMAgent against advanced proprietary models (e.g., GPT-4o [14]), state-of-the-art open-source models (e.g., LLaVAOneVision-7B [19], Qwen2.5-VL [2]), and models implementing multimodal CoT (e.g., Deep-

Table 2. Ablation experiments: “w/o MIFG-QA” refers to adopting only single-image training data, “w/o lookback” denotes not using visual reflection tools, and “w/o Traj mask” signifies not masking invalid tracks.

Components	V*			HR-Bench			MME	MIFG-QA		
	direct	relative	Avg	4K	8K	Avg		nature	poster	Avg
baseline	79.13	73.68	76.96	70.62	66.75	68.69	57.3	36.94	44.34	41.98
w/o MIFG-QA	<u>87.83</u>	80.26	<u>84.81</u>	<u>72.75</u>	70.5	71.63	64.02	39.90	40.18	40.09
w/o lookback	86.07	76.32	82.20	<b>74.0</b>	<u>71.25</u>	<b>72.63</b>	62.24	<u>48.25</u>	47.98	<u>48.07</u>
w/o Traj mask	86.09	<u>81.59</u>	84.29	73.5	69.75	71.63	64.03	46.31	46.18	46.23
IMAgent	<b>88.70</b>	<b>88.16</b>	<b>88.48</b>	<u>73.5</u>	<b>71.5</b>	<u>72.5</u>	<b>64.83</b>	<b>50.24</b>	<b>48.73</b>	<b>49.21</b>

eyes [67], Pixels Reasoner [35], Chain-of-Focus [63]).

For evaluation benchmarks, we perform comprehensive comparisons on three classic single-image fine-grained benchmarks (V\* Bench [47], HR-Bench [41], and MME-RealWorld [64]) and our proposed MIFG-QA -val to validate the effectiveness of IMAgent’s dynamic visual reasoning. The test data of V\* Bench and HR-Bench includes ultra-high-resolution images with resolutions ranging from 2k to 8k, where the target objects relevant to the test questions account for a very small proportion of pixels. Such extensive redundant visual information increases the difficulty for VLMs to accurately locate targets and answer questions. MME-RealWorld is a large-scale high-resolution dataset of real-world scenarios, covering 43 scenarios, which focuses on evaluating the perception and reasoning capabilities of multimodal large models.

## 4.2. Main Results

In Table 1 of the experimental results, we reveal a noteworthy phenomenon that, for base Qwen2.5-VL-7B, on V\* and HR-Bench, directly generated answer (row 6) is superior to the step-by-step generated ones (row 7), especially on the higher resolution tasks(HR-Bench 8K).

On our MIFG-QA, where the input images have relatively high total resolution and abundant fine-grained information, we observe a similar phenomenon. We speculate that this phenomenon stems from the issue revealed in Figure 1.

While existing methods achieve significant improvements in single-image scenarios through external visual tools, they largely overlook multi-image tasks—either lacking native support or failing to evaluate in such settings. To benchmark these vision agents on our proposed MIFG-QA-val, we modify prompts for models incompatible with multi-image operations, forcing them to output image indices during tool call.

IMAgent leverages visual reflection and confirmation mechanisms to autonomously prioritize critical images/regions, surpassing state-of-the-art workflow-based methods [20, 33, 47] and training-based approaches [35, 63, 67] by significant margins. Crucially, this gain requires neither

complex workflow design nor elaborate cold-start SFT, instead unlocking dynamic visual capabilities through end-to-end reinforcement learning.

Table 3. Model Performance Comparison Across Different Max-Pixels. MP means maxpixels of input image.

MP	Model	V*	HR-Bench		MME
			4K	8K	
12M	Qwen2.5-VL	76.96	70.62	66.75	57.3
	Pixel Reasoner	85.86	68.75	63.25	<u>64.41</u>
	Deepeyes	<u>87.96</u>	<b>75.0</b>	<u>69.75</u>	64.0
	Ours	<b>88.48</b>	<u>73.5</u>	<b>71.5</b>	<b>64.83</b>
4M	Qwen2.5-VL	75.39	69.75	64.25	56.76
	Pixel Reasoner	85.34	68.75	62.25	<u>63.91</u>
	Deepeyes	<u>87.96</u>	<b>73.0</b>	<b>67.75</b>	63.86
	ours	<b>88.48</b>	<u>71.5</u>	<u>66.12</u>	<b>64.33</b>
1M	Qwen2.5-VL	71.73	62.38	52.12	51.35
	Pixel Reasoner	77.49	<u>65.25</u>	55.12	<u>61.51</u>
	Deepeyes	<u>80.10</u>	<b>65.75</b>	<u>55.25</u>	60.23
	Ours	<b>80.62</b>	64.12	<b>55.62</b>	<b>61.67</b>

We also conducted inference experiments under limited-resolution scenarios, and the results are shown in Table 3. Experiments demonstrate that when the maximum input resolution decreases, the problem becomes more difficult. All models exhibit a downward trend in overall performance; however, models with multimodal CoT still retain their performance advantages, being significantly superior to base models. Furthermore, our model still performs excellently under constrained scenarios, which demonstrates the adaptability of IMAgent’s dynamic visual thinking.

## 4.3. Ablation Study

We further investigate the impacts of visual tools, training data, and trajectory masking on the model’s dynamic visual capabilities, with the results presented in Table 2.

A comparison between Row 3 and Row 5 demonstrates that when equipped with the visual reflection tool, the model’s overall performance (on the V\*, MME, and MIFG-QA datasets) is significantly improved, despite a potential

decrease on HR-Bench caused by the excessively high proportion of image tokens resulting from the reuse of high-resolution images. Explicit visual reflection enables the model to re-examine images, thereby achieving more precise alignment between questions and image regions. For multi-image scenarios, the reflection tool assists the model in identifying images relevant to the query.

Experiments in Row 2 and Row 5 show that incorporating multi-image data into the training process helps comprehensively enhance model performance. Multi-image data involves more image elements and comparisons between images, which effectively expands the diversity of tasks the model learns and encourages the model to explore richer tool use strategies. A comparison between Row 4 and Row 5 indicates that the model’s multi-image processing capability drops sharply if trajectory masking is not applied during training. Multi-image tasks typically require more visual operations and interaction rounds. The lack of masking for invalid trajectories inhibits long-range interactions, thus limiting the model’s exploration of tool-use strategies for multi-image problems during training.

In summary, the multi-image training data we add helps the model learn tool use methods in multi-image scenarios and improves its overall performance. The proposed visual reflection function allows the model to re-evaluate images. Filtering invalid trajectories expands the model’s tool exploration space and enhances its multi-image processing capability. The synergistic effect of these three components endows the model with dynamic visual thinking capabilities and boosts its overall performance.

## 5. Key Findings

### 5.1. Enabling Attention Reallocation via Visual Tools



Figure 5. Attention maps of the model using the visual confirmation tool. To the left of the blue dashed line are the query image pair, where the thumbnail in Text Box indicates the cropped region. To the right of the dashed line are the attention maps corresponding to one token each when the model outputs four bounding boxes.

Figure 1(a,b) show that the general-purpose vision model Qwen2.5-VL gradually stops attending to images in later reasoning steps, especially in multi-image tasks. The model “sees” the images only at the initial reasoning stage; thereafter, even when the reasoning involves image content, it fails to enhance attention focus on the corresponding image regions. This reliance solely on the visual “first impression” stems from the model’s training bias toward continuing reasoning based on already generated linguistic content rather than revisiting visual evidence. When facing complex visual scenarios, this often leads to performance degradation.

In contrast, experiments in Figure 1 (c, d) demonstrate that IMAgent, equipped with confirmation and reflection tools, can proactively revisit visual evidence. This enables it to maintain autonomous visual attention allocation throughout the entire reasoning process and achieve visual focus on key regions. Additionally, we observe that the model pays

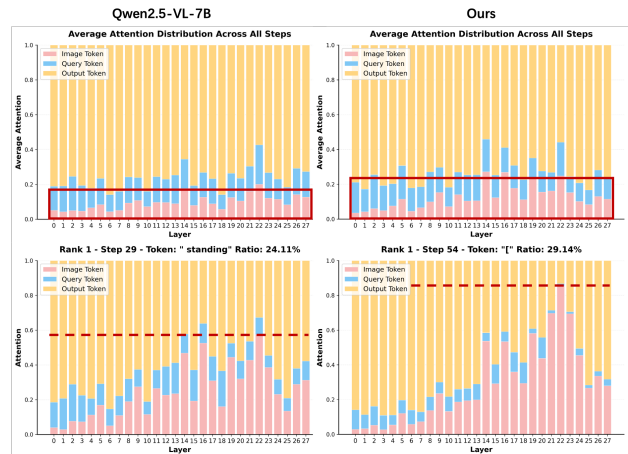


Figure 6. Attention distribution across model layers. The first row shows the layer-wise attention distribution of all output tokens to the three token categories. The second row presents the layer-wise attention distribution of the output tokens where the model’s attention to images reaches its peak.

higher attention to images when calling tools. These moments of heightened attention occur when the model outputs bounding boxes for the regions to be confirmed— corresponding to the shaded “[bounding box]” segments marked in Figure 1 (c). Figure 5 show that IMAgent highly focuses on the problem-related regions during bounding box output. This enhanced attention to images is primarily concentrated on image regions relevant to the problem, rather than being equally or similarly elevated across all regions.

We further analyze the attention distribution across all layers of the model during the entire reasoning process and at the moments of peak image attention, as shown in Figure 6. We found that higher image attention typically appears in the middle and later layers of the model, and IMAgent also exhibits significantly higher image at-

tion in these layers. This phenomenon is more pronounced in the comparison of attention distribution at the token level: IMAgent demonstrates far greater visual attention than Qwen2.5-VL across multiple intermediate layers.

## 5.2. The Importance of Tool Incentives for Zero RL

Our experiments demonstrate that providing tool incentives for agents under the Zero RL paradigm is critical. Figure 7 illustrates the impact of tool gains on the agent’s ability to master tool invocation. When the tool incentive is set to 0, although the system prompt encourages the model to explore visual tools initially, this exploration gradually diminishes to 0 as the number of training steps increases—with the model preferring to learn direct reasoning strategies instead. This phenomenon may arise from three factors: the base model, training characteristics, and training data. Specifically, instruction-tuned models such as Qwen2.5-VL-Instruct lack interactive data related to tool use in their training corpora, leading to poor tool interaction capabilities. Additionally, exploratory tool use by the model in the early training stages often results in inaccurate or inefficient tool calls; the subsequent format penalties and feedback from failed tool invocations inhibit further tool exploration. Furthermore, certain samples in the training data do not strictly require visual processing to generate correct responses, enabling the model to bypass tool use and directly obtain answers.

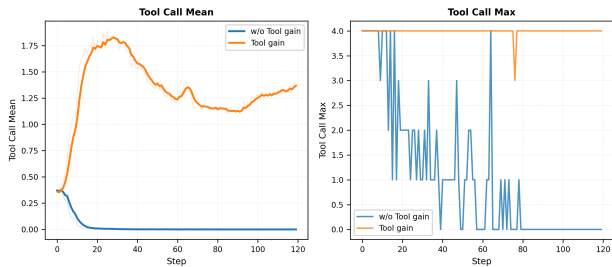


Figure 7. Comparison of tools with and without trajectory masks.

To address this, we design an accuracy-driven tool use gain incentive for IMAgent. This incentive encourages the model to learn strategies that utilize tools to achieve correct responses while avoiding meaningless tool use. After introducing the tool gain, the average number of tool uses per step by IMAgent gradually increases and reaches a peak in the early training phase—indicating that the tool gain effectively motivates the model to explore tool use initially. In the middle training phase, the average number of tool uses per step gradually decreases, reflecting that the model has adapted to completing visual reasoning tasks with tools and begins to shift toward more efficient tool use strategies. In the late training phase, the model masters several reasoning strategies integrated with tool use, and the average number

of tool uses per step exhibits a stable trend.

## 5.3. Zero RL inspires dynamic visual reasoning

Although IMAgent needs no SFT cold-start for memorizing specific reasoning pattern, end2end RL post-training still stimulates its dynamic visual reasoning ability. As shown in Figure 8, the model exhibits a usage pattern that prioritizes confirmation tools, supplemented by reflection tools, giving rise to diverse tool-use strategies exemplified by direct or exploratory visual confirmation, and cross-image comparative or reflective confirmation, among others.

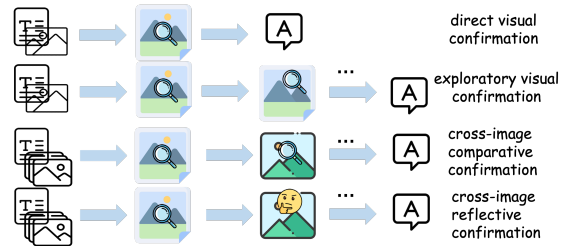


Figure 8. Demonstration of some typical tool use strategies.

For single-image questions, when the question involves a moderately sized image region, IMAgent tends to adopt direct visual confirmation. It provides an answer after invoking the confirmation tool once to obtain feedback. If the target region is small or involves multiple comparative regions, the model tends to explore the target region or perform confirmation one by one to acquire detailed information. In such cases, the model may also conduct summary reflection after confirmation to verify the answer. For multi-image questions, the frequency of reflection tool use is higher than that in single-image scenarios. After performing attention-focused confirmation operations, the model may forget details of other images. At this point, the model will select the reflection tool to reallocate visual attention for image information, and then choose the confirmation tool again or directly answer the question. More detailed examples of reasoning are shown in the appendix.

## 6. Conclusion

In this work, we present IMAgent, an open-source vision agent trained via pure end2end reinforcement learning to address complex single-image and multi-image tasks. By introducing a curated multi-image QA dataset, MIFG-QA, and equipping the agent with specialized tools for visual reflection and confirmation, our approach enables dynamic adjustment of image attention and stable tool use throughout reasoning. Extensive experiments show that IMAgent achieves state-of-the-art performance on both single-image and multi-image benchmarks, offering valuable insights and practical guidelines for advancing the development of vision agents in real-world scenarios.

## References

- [1] Deepak Bhaskar Acharya, Karthigeyan Kuppan, and B Divya. Agentic ai: Autonomous intelligence for complex goals—a comprehensive survey. *IEEE Access*, 2025. 1
- [2] Shuai Bai, Keqin Chen, Xuejing Liu, Jialin Wang, Wenbin Ge, Sibao Song, Kai Dang, Peng Wang, Shijie Wang, Jun Tang, et al. Qwen2. 5-vl technical report. *arXiv preprint arXiv:2502.13923*, 2025. 5
- [3] Meng Cao, Haoze Zhao, Can Zhang, Xiaojun Chang, Ian Reid, and Xiaodan Liang. Ground-r1: Incentivizing grounded visual reasoning via reinforcement learning. *arXiv preprint arXiv:2505.20272*, 2025. 1, 3
- [4] Jiajun Chai, Guojun Yin, Zekun Xu, Chuhuai Yue, Yi Jia, Siyu Xia, Xiaohan Wang, Jiwen Jiang, Xiaoguang Li, Chengqi Dong, Hang He, and Wei Lin. Rlfactory: A plug-and-play reinforcement learning post-training framework for llm multi-turn tool-use, 2025. 2
- [5] DeepSeek-AI. Deepseek-r1: Incentivizing reasoning capability in llms via reinforcement learning, 2025. 2
- [6] Yuhao Dong, Zuyan Liu, Hai-Long Sun, Jingkan Yang, Winston Hu, Yongming Rao, and Ziwei Liu. Insight-v: Exploring long-chain visual reasoning with multimodal large language models, 2025. 2
- [7] Jiazhan Feng, Shijue Huang, Xingwei Qu, Ge Zhang, Yujia Qin, Baoquan Zhong, Chengquan Jiang, Jinxin Chi, and Wanjun Zhong. Retool: Reinforcement learning for strategic tool use in llms, 2025. 3
- [8] Kaituo Feng, Kaixiong Gong, Bohao Li, Zonghao Guo, Yibing Wang, Tianshuo Peng, Junfei Wu, Xiaoying Zhang, Benyou Wang, and Xiangyu Yue. Video-r1: Reinforcing video reasoning in mllms, 2025. 2
- [9] Xingyu Fu, Minqian Liu, Zhengyuan Yang, John Corring, Yijuan Lu, Jianwei Yang, Dan Roth, Dinei Florencio, and Cha Zhang. Refocus: Visual editing as a chain of thought for structured image understanding. *arXiv preprint arXiv:2501.05452*, 2025. 1
- [10] Zhi Gao, Bofei Zhang, Pengxiang Li, Xiaojian Ma, Tao Yuan, Yue Fan, Yuwei Wu, Yunde Jia, Song-Chun Zhu, and Qing Li. Multi-modal agent tuning: Building a vlm-driven agent for efficient tool usage, 2025. 2
- [11] Xinyu Geng, Peng Xia, Zhen Zhang, Xinyu Wang, Qiuchen Wang, Ruixue Ding, Chenxi Wang, Jialong Wu, Yida Zhao, Kuan Li, Yong Jiang, Pengjun Xie, Fei Huang, and Jingtren Zhou. Webwatcher: Breaking new frontier of vision-language deep research agent, 2025. 3
- [12] Zhibin Gou, Zhihong Shao, Yeyun Gong, Yelong Shen, Yujia Yang, Minlie Huang, Nan Duan, and Weizhu Chen. Tora: A tool-integrated reasoning agent for mathematical problem solving, 2024. 3
- [13] Xiaojun Guo, Runyu Zhou, Yifei Wang, Qi Zhang, Chenheng Zhang, Stefanie Jegelka, Xiaohan Wang, Jiajun Chai, Guojun Yin, Wei Lin, and Yisen Wang. Ssl4rl: Revisiting self-supervised learning as intrinsic reward for visual-language reasoning, 2025. 2
- [14] Aaron Hurst, Adam Lerer, Adam P Goucher, Adam Perelman, Aditya Ramesh, Aidan Clark, AJ Ostrow, Akila Welihinda, Alan Hayes, Alec Radford, et al. Gpt-4o system card. *arXiv preprint arXiv:2410.21276*, 2024. 5
- [15] Dongzhi Jiang, Renrui Zhang, Ziyu Guo, Yanmin Wu, Jiayi Lei, Pengshuo Qiu, Pan Lu, Zehui Chen, Chaoyou Fu, Guanglu Song, Peng Gao, Yu Liu, Chunyuan Li, and Hongsheng Li. Mmsearch: Benchmarking the potential of large models as multi-modal search engines, 2024. 2
- [16] Dongzhi Jiang, Renrui Zhang, Ziyu Guo, Yanmin Wu, Jiayi Lei, Pengshuo Qiu, Pan Lu, Zehui Chen, Chaoyou Fu, Guanglu Song, et al. Mmsearch: Benchmarking the potential of large models as multi-modal search engines. *arXiv preprint arXiv:2409.12959*, 2024. 1
- [17] Bowen Jin, Hansi Zeng, Zhenrui Yue, Jinsung Yoon, Sercan Arik, Dong Wang, Hamed Zamani, and Jiawei Han. Search-r1: Training llms to reason and leverage search engines with reinforcement learning. *arXiv preprint arXiv:2503.09516*, 2025. 1
- [18] Xin Lai, Junyi Li, Wei Li, Tao Liu, Tianjian Li, and Hengshuang Zhao. Mini-o3: Scaling up reasoning patterns and interaction turns for visual search, 2025. 3
- [19] Bo Li, Yuanhan Zhang, Dong Guo, Renrui Zhang, Feng Li, Hao Zhang, Kaichen Zhang, Peiyuan Zhang, Yanwei Li, Ziwei Liu, et al. Llava-onevision: Easy visual task transfer. *arXiv preprint arXiv:2408.03326*, 2024. 5
- [20] Geng Li, Jinglin Xu, Yunzhen Zhao, and Yuxin Peng. Dyfo: A training-free dynamic focus visual search for enhancing llms in fine-grained visual understanding. In *Proceedings of the Computer Vision and Pattern Recognition Conference*, pages 9098–9108, 2025. 5, 6
- [21] Xuefeng Li, Haoyang Zou, and Pengfei Liu. Torl: Scaling tool-integrated rl, 2025. 3
- [22] You Li, Heyu Huang, Chi Chen, Kaiyu Huang, Chao Huang, Zonghao Guo, Zhiyuan Liu, Jinan Xu, Yuhua Li, Ruixuan Li, et al. Migician: Revealing the magic of free-form multi-image grounding in multimodal large language models. *arXiv preprint arXiv:2501.05767*, 2025. 1, 4
- [23] Yunxin Li, Zhenyu Liu, Zitao Li, Xuanyu Zhang, Zhenran Xu, Xinyu Chen, Haoyuan Shi, Shenyuan Jiang, Xintong Wang, Jifang Wang, Shouzheng Huang, Xinpeng Zhao, Borui Jiang, Lanqing Hong, Longyue Wang, Zhuotao Tian, Baoxing Huai, Wenhao Luo, Weihua Luo, Zheng Zhang, Baotian Hu, and Min Zhang. Perception, reason, think, and plan: A survey on large multimodal reasoning models, 2025. 2
- [24] Yiqing Liang, Jieli Qiu, Wenhao Ding, Zuxin Liu, James Tompkin, Mengdi Xu, Mengzhou Xia, Zhengzhong Tu, Laixi Shi, and Jiacheng Zhu. Modomodo: Multi-domain data mixtures for multimodal llm reinforcement learning, 2025. 2
- [25] Haowei Liu, Xi Zhang, Haiyang Xu, Yaya Shi, Chaoya Jiang, Ming Yan, Ji Zhang, Fei Huang, Chunfeng Yuan, Bing Li, et al. Mibench: Evaluating multimodal large language models over multiple images. *CoRR*, 2024. 1
- [26] Yuqi Liu, Bohao Peng, Zhisheng Zhong, Zihao Yue, Fanbin Lu, Bei Yu, and Jiaya Jia. Seg-zero: Reasoning-chain guided segmentation via cognitive reinforcement, 2025. 2

- [27] Ziyu Liu, Zeyi Sun, Yuhang Zang, Xiaoyi Dong, Yuhang Cao, Haodong Duan, Dahua Lin, and Jiaqi Wang. Visual-rl: Visual reinforcement fine-tuning, 2025. 2
- [28] Fanqing Meng, Lingxiao Du, Zongkai Liu, Zhixiang Zhou, Quanfeng Lu, Daocheng Fu, Tiancheng Han, Botian Shi, Wenhai Wang, Junjun He, Kaipeng Zhang, Ping Luo, Yu Qiao, Qiaosheng Zhang, and Wenqi Shao. Mm-eureka: Exploring the frontiers of multimodal reasoning with rule-based reinforcement learning, 2025. 2
- [29] OpenAI. Thinking with images. <https://openai.com/index/thinking-with-images/>, 2025. 1
- [30] Rafael Rafailov, Archit Sharma, Eric Mitchell, Stefano Ermon, Christopher D. Manning, and Chelsea Finn. Direct preference optimization: Your language model is secretly a reward model, 2024. 2
- [31] Rohit Saxena, Pasquale Minervini, and Frank Keller. Postersum: A multimodal benchmark for scientific poster summarization. *arXiv preprint arXiv:2502.17540*, 2025. 1, 4
- [32] Zhihong Shao, Peiyi Wang, Qihao Zhu, Runxin Xu, Junxiao Song, Xiao Bi, Haowei Zhang, Mingchuan Zhang, Y. K. Li, Y. Wu, and Daya Guo. Deepseekmath: Pushing the limits of mathematical reasoning in open language models, 2024. 2
- [33] Haozhan Shen, Kangjia Zhao, Tiancheng Zhao, Ruochen Xu, Zilun Zhang, Mingwei Zhu, and Jianwei Yin. Zoom-eye: Enhancing multimodal llms with human-like zooming capabilities through tree-based image exploration. In *Proceedings of the 2025 Conference on Empirical Methods in Natural Language Processing*, pages 6613–6629, 2025. 5, 6
- [34] Joykirat Singh, Raghav Magazine, Yash Pandya, and Akshay Nambi. Agentic reasoning and tool integration for llms via reinforcement learning. *arXiv preprint arXiv:2505.01441*, 2025. 1
- [35] Alex Su, Haozhe Wang, Weiming Ren, Fangzhen Lin, and Wenhui Chen. Pixel reasoner: Incentivizing pixel-space reasoning with curiosity-driven reinforcement learning. *arXiv preprint arXiv:2505.15966*, 2025. 1, 3, 5, 6
- [36] Zhaochen Su, Linjie Li, Mingyang Song, Yunzhuo Hao, Zhengyuan Yang, Jun Zhang, Guanjie Chen, Jiawei Gu, Juntao Li, Xiaoye Qu, et al. Openthinking: Learning to think with images via visual tool reinforcement learning. *arXiv preprint arXiv:2505.08617*, 2025. 1
- [37] Qwen Team. Qwen3-vl, 2025. 3
- [38] Chenyu Wang, Weixin Luo, Sixun Dong, Xiaohua Xuan, Zhengxin Li, Lin Ma, and Shenghua Gao. Mllm-tool: A multimodal large language model for tool agent learning, 2025. 2
- [39] Ke Wang, Houxing Ren, Aojun Zhou, Zimu Lu, Sichun Luo, Weikang Shi, Renrui Zhang, Linqi Song, Mingjie Zhan, and Hongsheng Li. Mathcoder: Seamless code integration in llms for enhanced mathematical reasoning, 2023. 3
- [40] Qiuchen Wang, Ruixue Ding, Yu Zeng, Zehui Chen, Lin Chen, Shihang Wang, Pengjun Xie, Fei Huang, and Feng Zhao. Vrag-rl: Empower vision-perception-based rag for visually rich information understanding via iterative reasoning with reinforcement learning, 2025. 3
- [41] Wenbin Wang, Liang Ding, Minyan Zeng, Xiabin Zhou, Li Shen, Yong Luo, Wei Yu, and Dacheng Tao. Divide, conquer and combine: A training-free framework for high-resolution image perception in multimodal large language models. In *Proceedings of the AAAI Conference on Artificial Intelligence*, pages 7907–7915, 2025. 6
- [42] Xiyao Wang, Zhengyuan Yang, Chao Feng, Yongyuan Liang, Yuhang Zhou, Xiaoyu Liu, Ziyi Zang, Ming Li, Chung-Ching Lin, Kevin Lin, Linjie Li, Furong Huang, and Lijuan Wang. Vicrit: A verifiable reinforcement learning proxy task for visual perception in vlms, 2025. 2
- [43] Ye Wang, Qianglong Chen, Zejun Li, Siyuan Wang, Shijie Guo, Zhirui Zhang, and Zhongyu Wei. Simple o3: Towards interleaved vision-language reasoning. *arXiv preprint arXiv:2508.12109*, 2025. 1
- [44] Yibin Wang, Zhimin Li, Yuhang Zang, Chunyu Wang, Qinglin Lu, Cheng Jin, and Jiaqi Wang. Unified multimodal chain-of-thought reward model through reinforcement fine-tuning, 2025. 2
- [45] Jinming Wu, Zihao Deng, Wei Li, Yiding Liu, Bo You, Bo Li, Zejun Ma, and Ziwei Liu. Mmsearch-rl: Incentivizing llms to search, 2025. 3
- [46] Mingyuan Wu, Jingcheng Yang, Jize Jiang, Meitang Li, Kaizhuo Yan, Hanchao Yu, Minjia Zhang, Chengxiang Zhai, and Klara Nahrstedt. Vtool-rl: Vlms learn to think with images via reinforcement learning on multimodal tool use. *arXiv preprint arXiv:2505.19255*, 2025. 1
- [47] Penghao Wu and Saining Xie. V?: Guided visual search as a core mechanism in multimodal llms. In *Proceedings of the IEEE/CVF Conference on Computer Vision and Pattern Recognition*, pages 13084–13094, 2024. 5, 6
- [48] Zijian Wu, Jinjie Ni, Xiangyan Liu, Zichen Liu, Hang Yan, and Michael Qizhe Shieh. Synthrl: Scaling visual reasoning with verifiable data synthesis, 2025. 2
- [49] Yuxi Xie, Anirudh Goyal, Wenyue Zheng, Min-Yen Kan, Timothy P. Lillicrap, Kenji Kawaguchi, and Michael Shieh. Monte carlo tree search boosts reasoning via iterative preference learning, 2024. 2
- [50] Guowei Xu, Peng Jin, Ziang Wu, Hao Li, Yibing Song, Lichao Sun, and Li Yuan. Llava-cot: Let vision language models reason step-by-step, 2025. 2
- [51] Haotian Xu, Xing Wu, Weinong Wang, Zhongzhi Li, Da Zheng, Boyuan Chen, Yi Hu, Shijia Kang, Jiaming Ji, Yingying Zhang, Zhijiang Guo, Yaodong Yang, Muhan Zhang, and Debing Zhang. Redstar: Does scaling long-cot data unlock better slow-reasoning systems?, 2025. 2
- [52] Shilin Xu, Yanwei Li, Rui Yang, Tao Zhang, Yueyi Sun, Wei Chow, Linfeng Li, Hang Song, Qi Xu, Yunhai Tong, Xiangtai Li, and Hao Fei. Mixed-rl: Unified reward perspective for reasoning capability in multimodal large language models, 2025. 2
- [53] Zhenghai Xue, Longtao Zheng, Qian Liu, Yingru Li, Xiaosen Zheng, Zejun Ma, and Bo An. Simpletir: End-to-end reinforcement learning for multi-turn tool-integrated reasoning. *arXiv preprint arXiv:2509.02479*, 2025. 5
- [54] Huanjin Yao, Jiaying Huang, Wenhao Wu, Jingyi Zhang, Yibo Wang, Shunyu Liu, Yingjie Wang, Yuxin Song, Haocheng Feng, Li Shen, and Dacheng Tao. Mulberry: Empowering mllm with o1-like reasoning and reflection via collective monte carlo tree search, 2024. 2

- [55] Tianyu Yu, Yuan Yao, Haoye Zhang, Taiwen He, Yifeng Han, Ganqu Cui, Jinyi Hu, Zhiyuan Liu, Hai-Tao Zheng, Maosong Sun, and Tat-Seng Chua. Rlhf-v: Towards trustworthy mlms via behavior alignment from fine-grained correctional human feedback, 2024. [2](#)
- [56] Chuhuai Yue, Jiajun Chai, Yufei Zhang, Zixiang Ding, Xihao Liang, Peixin Wang, Shihai Chen, Wang Yixuan, Wangyanping, Guojun Yin, and Wei Lin. UIOrchestra: Generating high-fidelity code from UI designs with a multi-agent system. In *Findings of the Association for Computational Linguistics: EMNLP 2025*, pages 2769–2782, Suzhou, China, 2025. Association for Computational Linguistics. [2](#)
- [57] Chuhuai Yue, Chengqi Dong, Yinan Gao, Hang He, Jiajun Chai, Guojun Yin, and Wei Lin. Promoting efficient reasoning with verifiable stepwise reward, 2025. [2](#)
- [58] Yufei Zhan, Yousong Zhu, Shurong Zheng, Hongyin Zhao, Fan Yang, Ming Tang, and Jinqiao Wang. Vision-r1: Evolving human-free alignment in large vision-language models via vision-guided reinforcement learning, 2025. [2](#)
- [59] Guibin Zhang, Hejia Geng, Xiaohang Yu, Zhenfei Yin, Zaibin Zhang, Zelin Tan, Heng Zhou, Zhongzhi Li, Xiangyuan Xue, Yijiang Li, et al. The landscape of agentic reinforcement learning for llms: A survey. *arXiv preprint arXiv:2509.02547*, 2025. [1](#)
- [60] Juntian Zhang, Song Jin, Chuanqi Cheng, Yuhan Liu, Yankai Lin, Xun Zhang, Yufei Zhang, Fei Jiang, Guojun Yin, Wei Lin, and Rui Yan. Viper: Empowering the self-evolution of visual perception abilities in vision-language model, 2025. [2](#)
- [61] Ruohong Zhang, Bowen Zhang, Yanghao Li, Haotian Zhang, Zhiqing Sun, Zhe Gan, Yinfei Yang, Ruoming Pang, and Yiming Yang. Improve vision language model chain-of-thought reasoning, 2024. [2](#)
- [62] Xintong Zhang, Zhi Gao, Bofei Zhang, Pengxiang Li, Xiaowen Zhang, Yang Liu, Tao Yuan, Yuwei Wu, Yunde Jia, Song-Chun Zhu, and Qing Li. Chain-of-focus: Adaptive visual search and zooming for multimodal reasoning via rl, 2025. [3](#)
- [63] Xintong Zhang, Zhi Gao, Bofei Zhang, Pengxiang Li, Xiaowen Zhang, Yang Liu, Tao Yuan, Yuwei Wu, Yunde Jia, Song-Chun Zhu, et al. Chain-of-focus: Adaptive visual search and zooming for multimodal reasoning via rl. *arXiv preprint arXiv:2505.15436*, 2025. [1](#), [3](#), [5](#), [6](#)
- [64] Yi-Fan Zhang, Huanyu Zhang, Haochen Tian, Chaoyou Fu, Shuangqing Zhang, Junfei Wu, Feng Li, Kun Wang, Qingsong Wen, Zhang Zhang, et al. Mme-realworld: Could your multimodal llm challenge high-resolution real-world scenarios that are difficult for humans? *arXiv preprint arXiv:2408.13257*, 2024. [6](#)
- [65] Yi-Fan Zhang, Xingyu Lu, Xiao Hu, Chaoyou Fu, Bin Wen, Tianke Zhang, Changyi Liu, Kaiyu Jiang, Kaibing Chen, Kaiyu Tang, Haojie Ding, Jiankang Chen, Fan Yang, Zhang Zhang, Tingting Gao, and Liang Wang. R1-reward: Training multimodal reward model through stable reinforcement learning, 2025. [2](#)
- [66] Jiaxing Zhao, Xihan Wei, and Liefeng Bo. R1-omni: Explainable omni-multimodal emotion recognition with reinforcement learning, 2025. [2](#)
- [67] Ziwei Zheng, Michael Yang, Jack Hong, Chenxiao Zhao, Guohai Xu, Le Yang, Chao Shen, and Xing Yu. Deep-eyes: Incentivizing” thinking with images” via reinforcement learning. *arXiv preprint arXiv:2505.14362*, 2025. [1](#), [3](#), [5](#), [6](#)
- [68] Hengguang Zhou, Xirui Li, Ruochen Wang, Minhao Cheng, Tianyi Zhou, and Cho-Jui Hsieh. R1-zero’s ”aha moment” in visual reasoning on a 2b non-sft model, 2025. [2](#)